European **J**ournal of **Chem**istry

Study on novel biphenyl chalcone scaffolds: A dual spectroscopic approach for efficient sensing of hydrazine with low concentration

Paresh Narayan Patel (iD) *, Shivani Nagindas Tandel (iD),
Amar Ghanshyam Deshmukh (iD) and Preksha Basant Patel (iD)

Laboratory of Bio-Organic Chemistry, Tarsadia Institute of Chemical Science (TICS), Uka Tarsadia University, Bardoli - 394 350, Gujarat, India

* Corresponding author at: Laboratory of Bio-Organic Chemistry, Tarsadia Institute of Chemical Science (TICS), Uka Tarsadia University, Bardoli - 394 350, Gujarat, India.
 e-mail: paresh.patel@utu.ac.in (P.N. Patel).

RESEARCH ARTICLE

ABSTRACT

Hydrazine and its derivatives, as harmful substances, seriously risk the health of humans and the environment. On the basis of the admirable luminescent properties and low biological harmfulness of the biphenyl moiety, a biphenyl moiety can be combined with a naphthalene ring via the chalcone scaffold easily traced by a nucleophilic group. Therefore, biphenyl chalcones (BPCs) decorated with various naphthalene systems as fluorescent sensors for hydrazine are synthesised by Claisen-Schmidt condensation. The present work describes the comparative studies of two different protocols for the synthesis of three different BPCs. The structures of all novel BPCs were investigated by FT-IR, NMR, and HRMS spectroscopy. These BPCs show a red shift with a fluorescent peak and an enhancement in intensity with increasing solvent polarity from hexane to methanol. Methanol shows strong fluorescence emission; therefore, methanol is used as the solvent in hydrazine sensing experiments. The BPCs display fluorescent variation from yellow to blue fluorescence after binding with hydrazine. These BPCs sensors are able to identify hydrazine in a fast response rate and 5 min response time. The screening study of hydrazine in various soil samples by prepared BPCs is highly efficient. A study of the pH dependence of these probes shows excellent sensitivity in the pH range of 5 to 10.

1. Introduction

Inorganic, colourless hydrazine is a highly toxic reducing chemical that is used as rocket fuel [1]. It can procedure liquid propellant with an oxidiser and is extensively used in attitude regulators of satellites and military missiles [2]. During World War II, German scientists used hydrazine for the first time as a fuel [3], and afterward hydrazine and its various derivatives prospered during the postwar era [4]. Due to the hypergolic propellant and a monopropellant nature [5,6], widespread acceptance of hydrazine was there as a consistent and potent propellant with liquid stuffs like water (Figure 1) [7].

Hydrazine is also known as a strong reducing agent and high alkalinity [8-10] for the synthesis of plastics, rubber foaming agents, isoniazid, and other drugs. It has also been used in the manufacture of polyamide and epoxy resin and other aspects [11-13]. Although these commercial advantages make it perfect for use in precise aerospace and rocket applications, hydrazine poses a danger to human environmental safety. It is miscible in polar solvents such as water and alcohol, and has saviour effects on human organs [14]. Hydrazine and its derivatives have a neurotoxic effect and due to their reducing ability, even small amounts of hydrazine can cause soft tissue injury, lung damage, seizures, coma, and death [15]. The dawn limit observed by the US Environmental Protection Agency is 10 ppb [16,17]. Therefore, it is vital to design a reliable, real-time, and effective method for the detection of even small amounts of hydrazine.
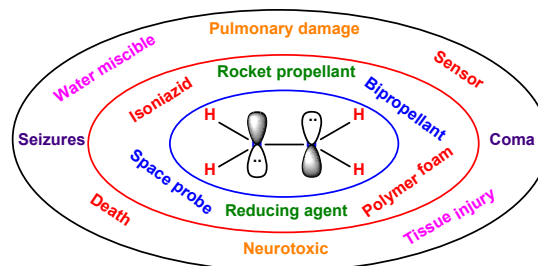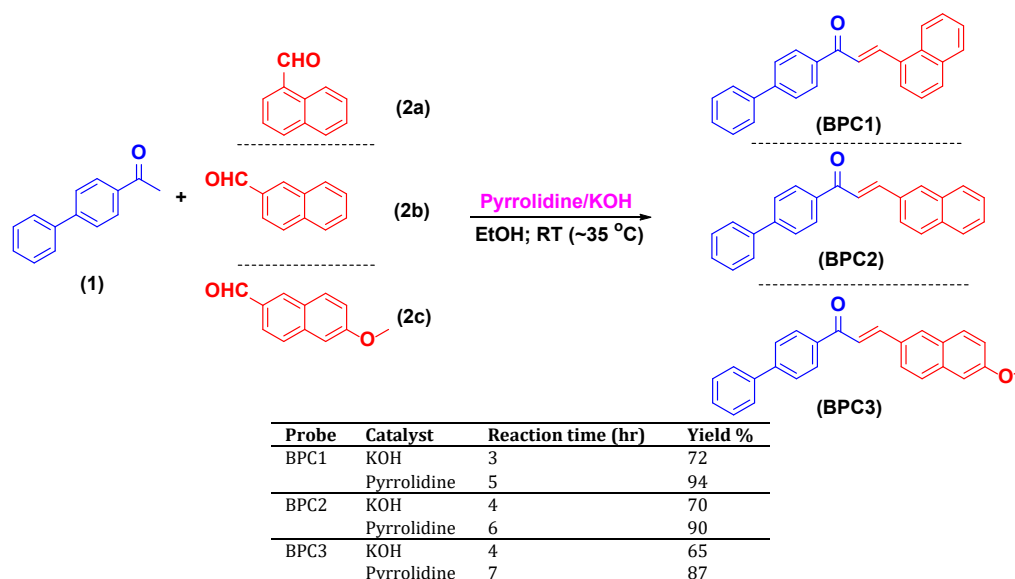

Figure 1. Hydrazine: A privileged structure in chemical sciences.

Certain detection approaches based on the basicity and nucleophilicity of hydrazine have been reported, including the cleavage type [18-22], nucleophilic addition reaction [23-25], and the nucleophilic cascade reaction [26-30].

Scheme 1. The synthetic route of probe BPCs.

Probe	Catalyst	Reaction time (hr)	Yield %
BPC1	KOH	3	72
	Pyrrolidine	5	94
BPC2	KOH	4	70
	Pyrrolidine	6	90
BPC3	KOH	4	65
	Pyrrolidine	7	87

A ratiometric fluorescent sensor of coumarin chalcone for hydrazine with cyclization reaction has been reported [31,32]. Therefore, on the basis of the robust fluorescence properties of the biphenyl group connected with the typical hydrazine detection group, chalcone, biphenyl chalcone derivatives (BPCs) decorated by various naphthalene terminal groups as fluorescent sensors for hydrazine are developed, studied, and presented here. BPCs have identified hydrazine by UV-vis absorption and fluorescence emission studies with a low exposure limit, good selectivity, and a fast response rate.

2. Experimental

2.1. General information and material

All chemicals were obtained from Sigma-Aldrich and used without further purification. Solvents were dried over molecular sieves if necessary. The ^{1}H, H-H Cosy and HETCOR, ^{13}C NMR spectra were recorded in CDCl$_3$ or DMSO-d_6 at room temperature using a Bruker Avance III 500 MHz (AV 500) NMR spectrometer, and TMS was used as an internal reference standard. Infrared (IR) spectra were recorded neat by ATR on a Thermo Nicolet iS50 FT-IR spectrometer and are reported in cm^{-1}. HR-MS data were obtained in a methanol with Thermo Scientific Orbitrap Elite mass spectrometer. The melting points were measured by an open capillary method using the Sigma melting point apparatus. Single-crystal structural data were recorded on a Bruker Kappa APEXII. High-performance liquid chromatography (HPLC) was performed on JASCO instruments at 210 nm using Daicel CHIRALCEL OJ-H 4.6 mm × 25 cm. Optical rotations were measured on a Rudolph Autopol IV digital polarimeter. For thin layer chromatography (TLC) analysis throughout this work, Merck precoated TLC plates (silica gel 60 GF$_{254}$, 0.25 mm) were used. The products were purified by recrystallisation or column chromatography on silica gel 60 (Merck, 230-400 mesh).

2.2. General process for synthesis of probes BPCs

To a stirred solution of 1-([1,1'-biphenyl]-4-yl)ethan-1-one (1) (1.62 g, 10 mmol) in ethanol (5 mL), the naphthaldehyde derivatives (2a-c) (10 mmol) dissolved in ethanol (2-3 mL) was added portion wise (Scheme 1). The reaction mixture was stirred at room temperature for 20 min, during which it turned to a homogeneous solution. Then a catalytic amount of KOH/ pyrrolidine was added and the resultant mixture was stirred at room temperature for 2-3/5-6 h. The reaction was monitored on TLC. After completion of the reaction, the precipitated products of BPCs were collected by filtration. The crude product was purified by recrystallisation from CHCl$_3$: MeOH (1:1, *v/v*, 10 mL) to afford (65-72/87-94 % yield) the product as yellow to light brown color (BPC1-BPC3).

(E)-3-([1,1'-biphenyl]-4-yl)-1-(naphthalen-1-yl)prop-2-en-1-one (BPC1): Color: Yellow solid. Yield: 80/92 % (KOH/ Pyrrolidine). M.p.: 158-160 °C. FT-IR (KBr, ν, cm^{-1}): 1708 (C=O) (ketone), 1624 (C=C) (propene). ^{1}H NMR (500 MHz, DMSO-d_6, δ, ppm): 8.73 (d, *J* = 15.5 Hz, 1H, α-H), 8.31 (d, *J* = 8.5 Hz, 1H, Ar-H), 8.19 (d, *J* = 8.5 Hz, 2H, Ar-H), 7.97-7.92 (m, 3H, Ar-H), 7.78 (d, *J* = 8.5 Hz, 2H, Ar-H), 7.72 (s, 1H, Ar-H), 7.70-7.68 (m, 2H, Ar-H, β-H), 7.65-7.61 (m, 1H, Ar-H), 7.59-7.55 (m, 2H, Ar-H), 7.53-7.50 (m, 2H, Ar-H), 7.44 (tt, *J* = 7.5, 2.0 Hz, 1H, Ar-H). ^{13}C NMR (125 MHz, DMSO-d_6, δ, ppm): 189.77 (C=O), 145.65 (Ar-C), 141.70 (Ar-C), 139.96 (Ar-C), 136.90 (Ar-C), 133.78 (Ar-C), 132.47 (Ar-C), 131.81 (Ar-C), 130.83 (Ar-C), 129.23 (Ar-C), 128.98 (Ar-C), 128.78 (Ar-C), 128.25 (Ar-C), 127.36 (Ar-C), 127.32 (Ar-C), 127.01 (Ar-C), 126.34 (Ar-C), 125.47 (Ar-C), 125.13 (Ar-C), 124.69 (Ar-C), 123.56 (Ar-C). HRMS (ESI, Ion Trap, *m/z*) [M+H]: Calculated (C$_{25}$H$_{18}$O) 334.1400, Observed 335.1552. HPLC (Isocratic; ACN:H$_2$O 85:15, 30 min; Flow 1 mL/min): r.t. 12.80 min, purity = 98.12 %.

(E)-3-([1,1'-biphenyl]-4-yl)-1-(naphthalen-2-yl)prop-2-en-1-one (BPC2): Color: Yellow solid. Yield: 84/95 % (KOH/ Pyrrolidine). M.p.: 178-180 °C. FT-IR (KBr, ν, cm^{-1}): 1689 (C=O) (ketone), 1605 (C=C) (propene). ^{1}H NMR (500 MHz, DMSO-d_6, δ, ppm): 8.57 (d, *J* = 0.5 Hz, 1H, Ar-H), 8.12 (dd, *J* = 8.5, 8.5 Hz, 2H, Ar-H), 8.03 (d, *J* = 7.5 Hz, 2H, Ar-H), 7.98 (d, *J* = 8.5 Hz, 1H, Ar-H), 7.94 (d, *J* = 8.5 Hz, 1H, Ar-H), 7.87 (d, *J* = 16, 1H, β-H), 7.81-7.79 (m, 3H, Ar-H+ α-H), 7.78 (s, 1H, Ar-H), 7.76-7.74 (dd, *J* = 6.5, 7 Hz, 2H, Ar-H), 7.68-7.64 (m, 2H, Ar-H), 7.63-7.59 (m, 2H, Ar-H). ^{13}C NMR (125 MHz, DMSO-d_6, δ, ppm): 189.49 (C=O), 142.02 (Ar-C), 139.30 (Ar-C), 135.70 (Ar-C), 135.00 (Ar-C), 132.72 (Ar-C), 132.53 (Ar-C), 130.24 (Ar-C), 129.58 (Ar-C), 128.85 (Ar-C), 127.91 (Ar-C), 128.85 (Ar-C), 127.91 (Ar-C), 127.02 (Ar-C), 125.09 (Ar-C), 124.30 (Ar-C), 118.42 (Ar-C), 113.52 (Ar-C). HRMS (ESI, Ion Trap, *m/z*): [M+H]: Calculated (C$_{25}$H$_{18}$O) 334.1400, Observed 335.1592. HPLC (Isocratic; ACN:H$_2$O 85:15, 30 min; Flow 1 mL/min): r.t. 13.28 min, purity = 97.30 %.
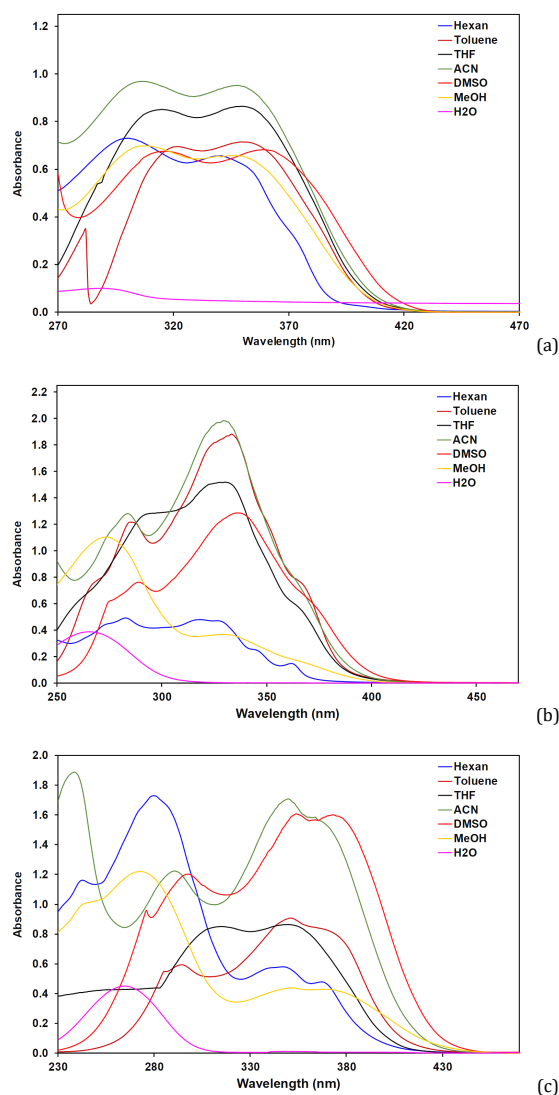
Figure 2. UV-vis absorption spectra of (a) BPC1, (b) BPC2, and (c) BPC3 in various solvents with 10 µM concentration.

(E)-3-([1, 1'-biphenyl]-4-yl)-1-(6-methoxynaphthalen-2-yl) prop-2-en-1-one (BPC3): Color: Yellow solid. Yield: 74/90 % (KOH/Pyrrolidine). M.p.: 212-214 °C. ^{1}H NMR (500 MHz, DMSO-d_6, δ, ppm): 8.17 (d, *J* = 10.5 Hz, 2H, Ar-H), 8.04-8.00 (m, 2H, Ar-H), 7.83-7.76 (m, 5H, Ar-H + β-H), 7.70-7.66 (m, 3H, Ar-H + α-H), 7.51 (t, *J* = 10.0 Hz, 2H, Ar-H), 7.43 (t, *J* = 9.0, 1H, Ar-H), 7.23.-7.17 (m, 2H, Ar-H), 3.98 (s, 3H, OCH$_3$). ^{13}C NMR (125 MHz, DMSO-d_6, δ, ppm): 189.96 (C=O), 158.97 (Ar-C), 145.42 (Ar-C), 145.15 (Ar-C), 140.01 (Ar-C), 137.14 (Ar-C), 135.91 (Ar-C), 130.55 (Ar-C), 130.25 (Ar-C), 129.11 (Ar-C), 128.96 (Ar-C), 128.77 (Ar-C), 128.18 (Ar-C), 127.54 (Ar-C), 127.30 (Ar-C), 124.42 (Ar-C), 121.06 (Ar-C), 119.53 (Ar-C), 106.04 (Ar-C), 55.41 (OCH$_3$). HRMS (ESI, Ion Trap, *m/z*) [M+H]: Calculated (C$_{26}$H$_{20}$O$_2$) 364.1500, Observed 365.0452. HPLC (Isocratic; ACN:H$_2$O 85:15, 30 min; Flow 1 mL/min): r.t. 10.74 min, purity = 95.70 %.

2.3. Photophysical properties and response to hydrazine

Stock solutions of all BPCs (5 mg) were prepared in different HPLC-grade solvents (5 mL). Working solutions of all BPCs with 5 µM concentrations for the investigation of UV-Vis absorption (Shimadzu UV-1900i spectrophotometer) and fluorescence emission (Shimadzu RF-6000 fluorescence spectrometer) investigation were prepared by serial dilution in respective HPLC-grade solvents. Both spectral titrations were carried out in methanol with 5 µM concentration of BPCs vs various concentrations of hydrazine. A representative competitive selectivity with different analytes, pH dependence and different types of soils studies for BPC3 were carried out in methanol with a 5 µM concentration.

3. Results and discussion

3.1. Synthesis of novel biphenyl chalcone (BPCs) probes

Initially, all probes were prepared by our earlier developed KOH catalyzed process [32-34]. Thereafter, to have the comparative investigation, we tried to prepare the same probes with the use of pyrrolidine as a catalyst by keeping the remaining parameters same. During this study, it was very much clearly observed that pyrrolidine is an effective alternative of KOH. In the case of KOH catalyzed process, we were able to complete the reaction in a short time but with significantly low yield compared to pyrrolidine. This could be because of the strong alkaline nature of KOH. The structures of all synthesized probes were confirmed by IR, NMR, and mass spectral analysis. The spectral data and illustrations have been presented in supporting information.
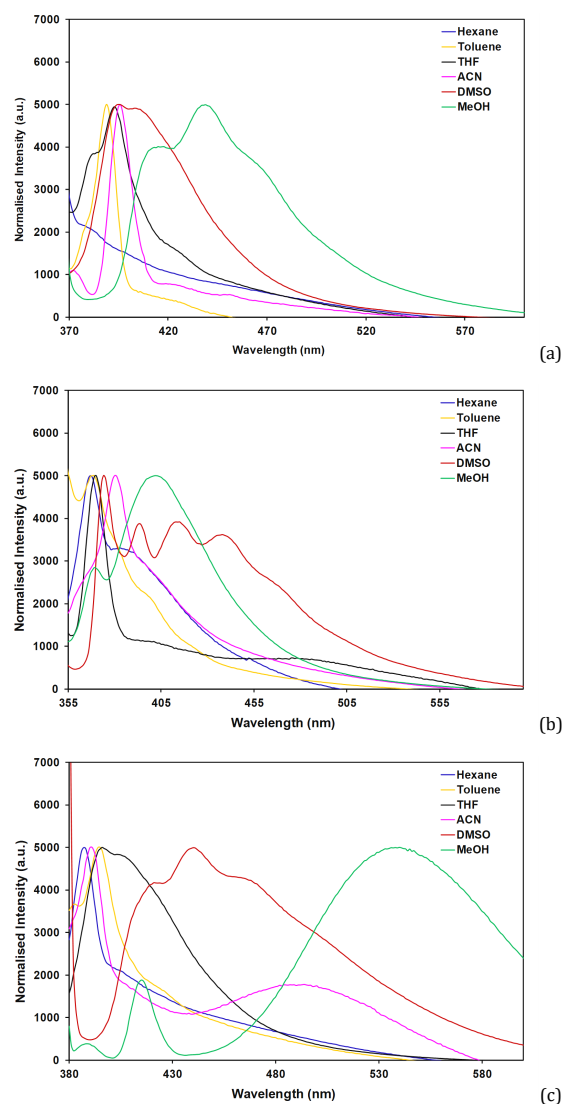
Figure 3. Normalised fluorescence spectra of (a) BPC1, (b) BPC2, and (c) BPC3 in various solvents with 5 µM concentration.

3.2. Photophysical properties of the probes

First, the photophysical natures of the probes in various solvents with various polarities were explored and the corresponding absorption spectra are shown in Figure 2. The absorption spectra of BPC1 in various solvents except that in water are similar with a main absorption peak at ~310 nm and a shoulder absorption peak at ~350 nm. The longer absorption peaks (vibrated structure at 315 and 345 nm) in acetonitrile and lower absorbance (at 300 nm, $\varepsilon = 2.65 \times 10^{-4}$ cm^{-1}M^{-1}) of the BPC1 probe in water may be derived from its poor solubility. Similarly, the absorption spectra of BPC2 in various solvents, except that in water and MeOH (main absorption peak at ~280 nm) are similar to the main absorption peak at ~345 nm. The longer absorption peak at 345 nm in acetonitrile and the lower absorbance (at 280 nm, $\varepsilon = 1.35 \times 10^{-4}$ cm^{-1}M^{-1}) of the BPC2 probe in water are also due to its poor solubility. The absorption spectra of BPC3 in various solvents except that in water (main absorption peak at ~250 nm) have a main absorption peak in the range of 250 to 390 nm. The longer absorption peak at 350 nm in acetonitrile and the lower absorbance (at 250 nm, $\varepsilon = 1.35 \times 10^{-4}$ cm^{-1}M^{-1}) of BPC3 probe in water is due to its solubility difference.

Thereafter, the photophysical properties of these probes in various solvents with various polarities were also studied by emission spectra as presented in Figure 3. The fluorescence spectra were normalised to compare the changes of fluorescence peak position more clearly with the solvent polarity. As expected, with the increase of the solvent polarity, the fluorescence peak positions of all probes have shown an obvious red shift up to 100 nm from hexane to methanol. This red shift was observed more in the case of BPC3, which could be due to the presence of the methoxy group. Their fluorescent colour can also achieve a corresponding change from blue to orange-red. On the basis of the fluorescence emission of all probes in methanol that was better than that in other solvents, the test environment for the identification properties of hydrazine was carried out in methanol. The results obtained show that the probe detection is also dependent on the solvent-salute interaction.

3.3. Titration experiment

The UV-Vis absorption titration spectra (concentration 10 µM) are shown in Figure 4. The absorption peaks of the compound BPC1 itself at 310 nm ($\varepsilon = 2.00 \times 10^{-4}$ cm^{-1}M^{-1}) and 350 nm ($\varepsilon = 1.68 \times 10^{-4}$ cm^{-1}M^{-1}) gradually increase and decrease, respectively, with continuous addition of hydrazine. At equal weight, the ration of BCP1/NH$_2$NH$_2$ absorption peak at 350 nm completely disappeared.
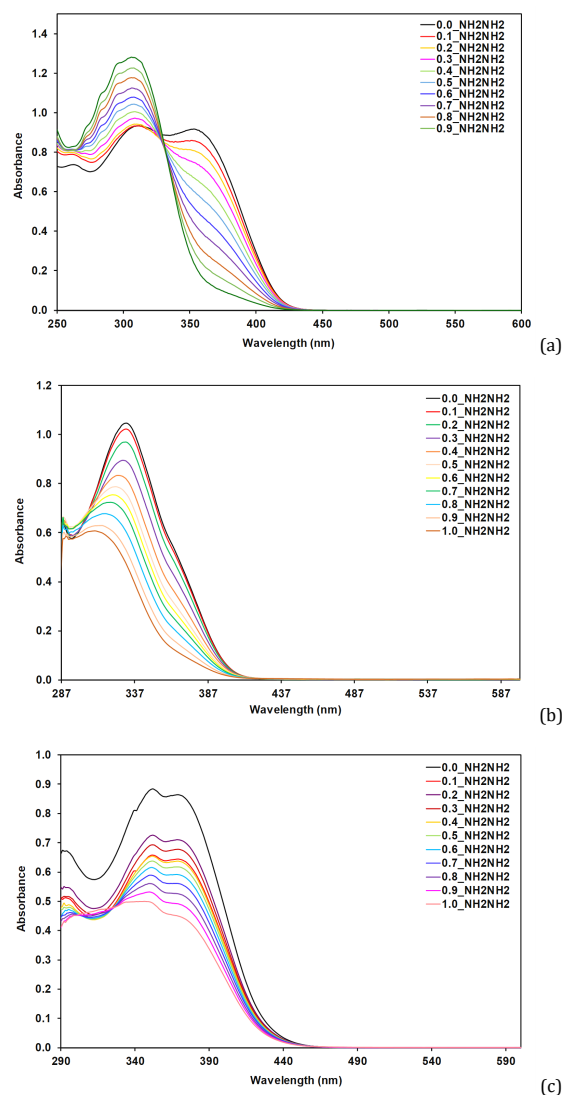
Figure 4. UV-Vis absorption spectra of the 10 μM probe BPC1 (a), BPC2 (b) and BPC3 (c) solution in MeOH after the addition of hydrazine.

The absorption peak at 310 nm was with the highest absorption. The colour changes from light yellow to colourless. This shows that the CBP1 probe can be used as a naked eye probe of hydrazine. In the case of BPC2, the absorption peak of at 335 nm (ε = 1.87×10^{-4} cm^{-1}M^{-1}) gradually decreases with continuous addition of hydrazine. In addition, there was a blue shift by a continuous decrease in wavelength by 25 nm. The equal weight ration of the absorption peak of BCP2 / NH2NH2 was shifted to 310 nm. The colour change from light yellow to colourless was also there in BPC2. This shows that the CBP2 probe can also be used as a naked eye probe of hydrazine. The continuous addition of hydrazine to the probe solution BPC3 has shown a gradual decrease in absorption peaks at 350 nm (ε = 1.78×10^{-4} cm^{-1}M^{-1}) and 368 nm (ε = 1.54×10^{-4} cm^{-1}M^{-1}). However, there was no significant colour change after the titration was complete.

The BPC1 probe itself presents an obvious fluorescence peak at 500 nm, which corresponds to bright yellow fluorescence under the fluorescent lamp. The addition of hydrazine leads to a decrease in the fluorescence peak at 500 nm (Figure 5, λ_{ex} = 350 nm). With increasing hydrazine, a new peak of the fluorescence signal at 400 nm appears and continuously increases under the excitation of 350 nm (Figure 3). In addition, the fluorescence colour before and after titration changes from bright yellow to blue-purple.

The BPC2 probe shows a minor fluorescence peak at 490 nm, which corresponds to the light-yellow fluorescence under the fluorescent lamp. The addition of hydrazine leads to a decrease in the fluorescence peak at 490 nm (Figure 5, λ_{ex} = 330 nm). With increasing hydrazine, a new peak of the fluorescence signal appears at 410 nm and continuously increases under 330 nm excitation (Figure 3). The fluorescence colour before and after titration changes from light yellow to light purple (concentration 5 μM).

The BPC3 probe shows a major fluorescence peak at 538 nm, which corresponds to the light orange fluorescence under the fluorescent lamp. The addition of hydrazine leads to a decrease in the fluorescence peak at 538 nm (Figure 5, λ_{ex} = 368 nm). The fluorescence colour before and after titration changes from light orange to light blue. Visible changes in fluorescence colour in all three probes show that these probes achieve a ratiometric fluorescent detection for hydrazine. Selectively, the fluorescence detection limit of BPC3 [35] was calculated based on the fluorescence intensity at 538 nm as 1.4 nM. This result shows that BPC3 is very sensitive for the detection of hydrazine in the nanomolar range. The results indicate that the probe BPC3 can be used for real-time detection of hydrazine in environment.
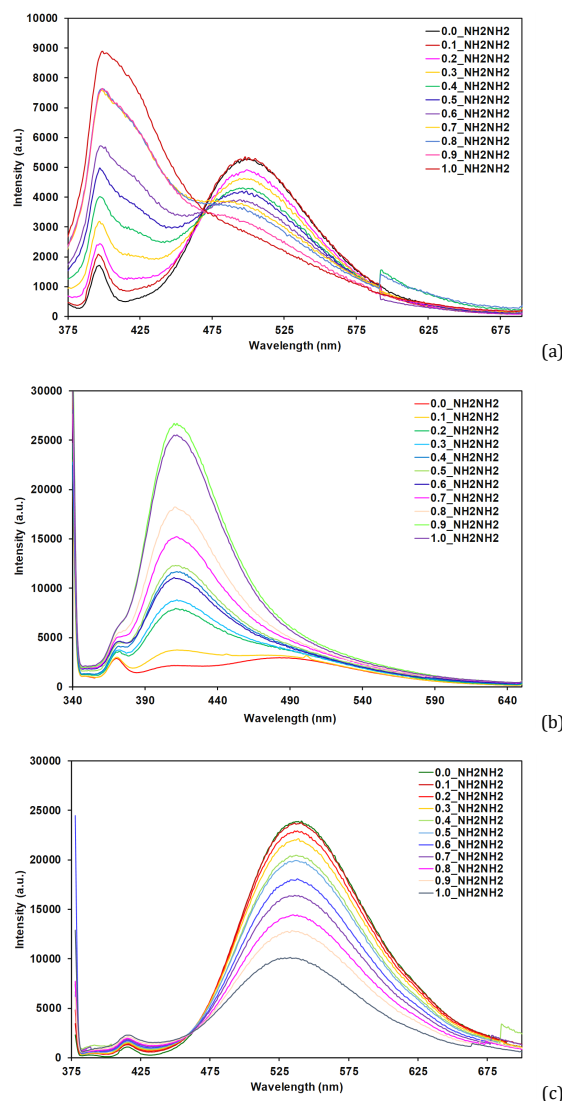
Figure 5. Fluorescence spectra of the 5 µM probes BPC1 (a), BPC2 (b), and BPC3 (c) solution in MeOH after the addition of hydrazine.

Furthermore, the time-dependent test of PBC on hydrazine (Figure 5) indicates that with an increase in time, the fluorescence intensity at 538 nm continues to decrease and reaches the ground around 15 min. The developed method and the results obtained are comparable with those of the existing literature. [31]

3.4. Investigation of the sensing mechanism

In order to study the chemical reaction involve sensing of hydrazine by BPCs, a mechanistic investigation is performed. In this study, a probe solution in methanol was injected into LC-MS before (BPC 10 µL) and after (BPC 10 µL + NH₂NH₂ 10 µL) sensing studies (Figure 6).

The BPC1 solution injected before the addition of hydrazine shows a molar ion peak at 335.1552 *m/z* corresponding to the hydrogen adduct of BPC1. However, a solution of BPC1 injected after 15 minutes of hydrazine addition shows a major molar ion peak at 347.1632 *m/z* corresponding to the pyrazole derivative of BPC1. This study shows that the hydrazine detection is occurring in 15 minutes and through the reaction shown in Scheme 2.

3.5. The practical applications of the probe (Selectively BPC3)

Discrimination, anti-interference, and pH obligations are prerequisites for a probe in the material application. Therefore, a competitive selectivity experiment of the BPC3 probe was conducted for other interference substances, including metal ions, anions, amines, and biological species (Figure 6). Apparently, BPC3 as a fluorescent probe for hydrazine has outstanding discrimination and antiinterference. The pH-dependent experiment of the BPC3 probe (Figure 6) indicates that the probe has excellent recognition properties for hydrazine in the pH range of 5-10.

The application of the BPC3 probe in the recognition of hydrazine in soils [37,38] was also examined. First, 1 g of field soil/clay soil/sandy soil was added to the BPC3 solution (10 µM), bright orange fluorescence was observed under a 365 nm UV lamp (Figure 8), which indicated that the analytes in the soil did not affect the fluorescence properties of BPC3. The fluorescence spectra of the supernatants were also measured (Figure 8), which shows that there was no major effect of different soil samples on the emission of BPC3. In the second experiment, 1 g of field soil/clay soil/sand soil was treated with hydrazine and then the soil was added to the solution of BPC3 (10 µM).
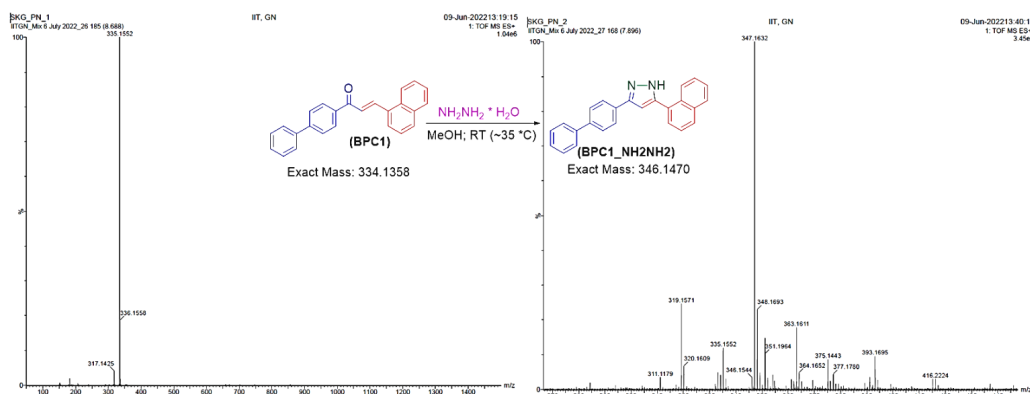
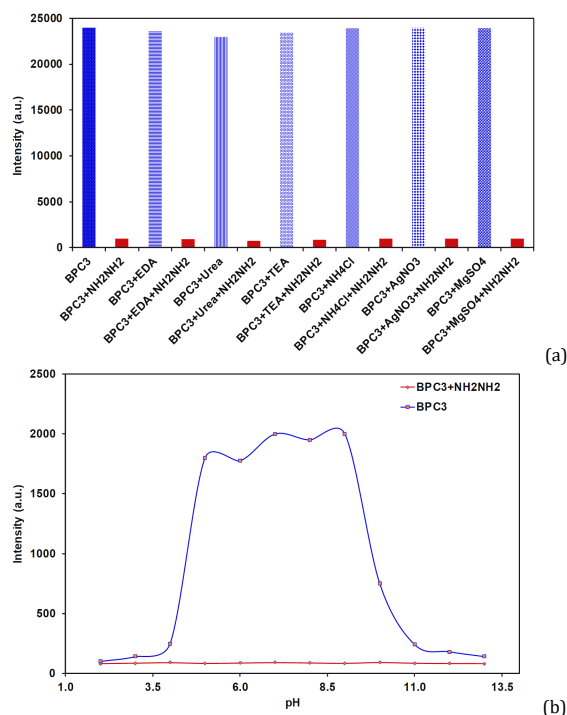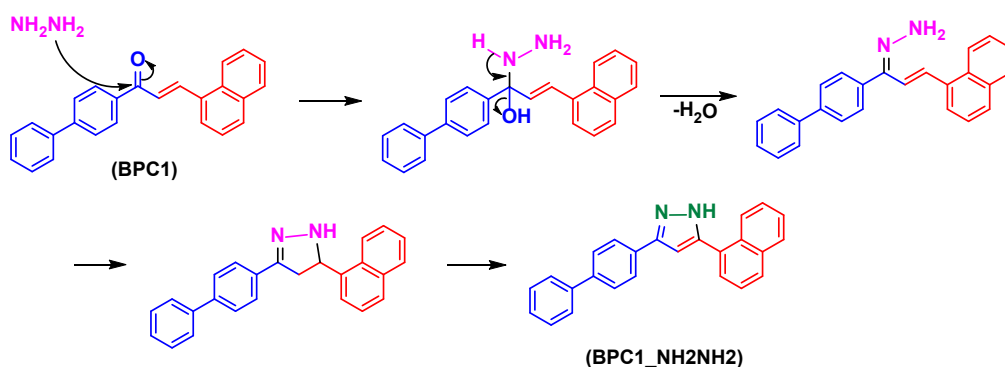**Figure 6.** HRMS of probe BPC1 before and after hydrazine addition.

Figure 7. (a) Competitive selectivity of BPC3 (5 µM; 538 nm) to different analytes; (b) pH dependence of BPC3 (5 µL; 538 nm).

Scheme 2. The mechanistic route of the hydrazine sensing study.

The solutions exhibit light blue fluorescence under a 365 nm UV lamp. The fluorescence spectra of the supernatants had shown a major decrease in the emission of BPC3.

On the basis of the quick response time, profound detection performance, outstanding selectivity, and antiinterference of probe BPCs, the detection effect of the probe on hydrazine in actual water samples may further be explored. We know that water contains some minerals including Na^+, Mg^{2+}, Fe^{3+}, Cu^{2+}, ClO^- and so on. According to the competitive selectivity (Figure 8), these substances do not interfere with the recognition of BPC3 in hydrazine.
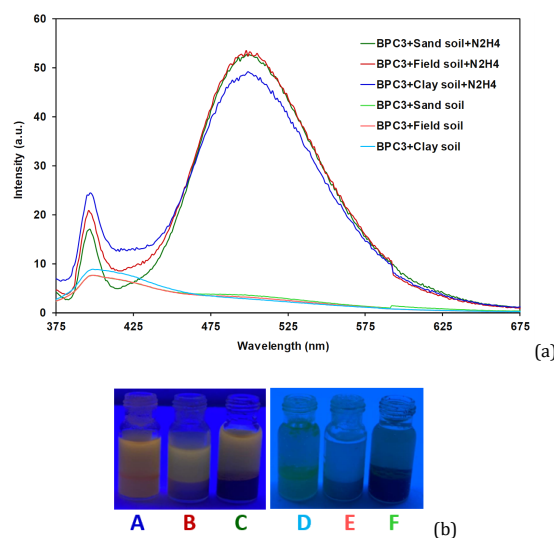
Figure 8. (a) Photographs and fluorescence spectra of the BPC3 probe (0.5 μM; 538 nm) after the addition of different soils in methanol with and without NH_2NH_2. (b) A & D sand soil, B & E field soil, C & F clay soil, before & after addition of hydrazine, respectively.

According to the pH dependence, the probe has excellent recognition properties for hydrazine in the pH range of 5-10. These probes may have excellent recognition for hydrazine in real water samples.

4. Conclusions

In summary, biphenyl fluorescent probes for hydrazine were synthesised by attaching chalcone with various naphthalene moieties to accelerate the sensing rate through pyrazole ring formation. Probable detection mechanisms of hydrazine follow the subsequent addition, cyclization processes forming a dihydropyrazole ring. The probe successfully realises the ratiometric identification for hydrazine with a detection limit of 1.4 nM, good selectivity, and anti-interference. Compared to the other hydrazine probes, these probes have a fast response rate with a reaction complete in 15 min. As a real-time application, the prepared probes can successfully detect hydrazine in different soil samples. A study of the pH dependence of the probe has shown excellent sensitivity in the pH range of 5 to 10. On the basis of these studies, a real-time hydrazine detection device can be developed from the prepared probes.

Acknowledgements

Disclosure statement DS

Conflict of interest: The authors declare that they have no conflict of interest.
Ethical approval: All ethical guidelines have been adhered to.
Sample availability: Samples of the compounds are available from the author.

Funding $

CRediT authorship contribution statement CR

Conceptualization: Paresh Patel; Methodology: Preksha Patel, Amar Deshmukh, Shivani Tendal; Software: Paresh Patel, Amar Deshmukh, Shivani Tendal; Validation: Paresh Patel; Formal Analysis: Amar Deshmukh, Shivani Tendal; Investigation: Paresh Patel, Amar Deshmukh, Shivani Tendal; Resources: Paresh Patel; Data Curation: Paresh Patel, Amar Deshmukh, Shivani Tendal; Writing - Original Draft: Preksha Patel, Amar Deshmukh, Shivani Tendal; Writing - Review and Editing: Paresh Patel; Visualization: Preksha Patel, Amar Deshmukh, Shivani Tendal; Funding acquisition: Paresh Patel, Amar Deshmukh, Shivani Tendal; Supervision: Paresh Patel; Project Administration: Paresh Patel.

ORCID iD and Email ✉

Paresh Narayan Patel
✉ pareshn111@yahoo.com
✉ paresh.patel@utu.ac.in
iD https://orcid.org/0000-0002-8514-4753
Shivani Nagindas Tandel
✉ shivanitandel1929@gmail.com
iD https://orcid.org/0000-0002-3533-2545
Amar Ghanshyam Deshmukh
✉ amudeshmukh93@gmail.com
iD https://orcid.org/0000-0002-9851-8953
Preksha Basant Patel
✉ prekshabpatel99@gmail.com
iD https://orcid.org/0000-0001-5451-7281

References

[1]. Nguyen, K. H.; Hao, Y.; Chen, W.; Zhang, Y.; Xu, M.; Yang, M.; Liu, Y.-N. Recent progress in the development of fluorescent probes for hydrazine. *Luminescence* **2018**, *33*, 816–836.

[2]. Zelnick, S. D.; Mattie, D. R.; Stepaniak, P. C. Occupational exposure to hydrazines: treatment of acute central nervous system toxicity. *Aviat. Space Environ. Med.* **2003**, *74*, 1285–1291.

[3]. Troyan, J. E. Properties, production, and uses of hydrazine. *Ind. Eng. Chem.* **1953**, *45*, 2608–2612.

[4]. Dambrauskas, T.; Cornish, H. H. The distribution, metabolism, and excretion of hydrazine in rat and mouse. *Toxicol. Appl. Pharmacol.* **1964**, *6*, 653–663.

[5]. Davis, S. M.; Yilmaz, N. Advances in hypergolic propellants: Ignition, hydrazine, and hydrogen peroxide research. *Adv. Aerosp. Eng.* **2014**, *2014*, 1–9.

[6]. Wang, Y.-H.; Jiang, S.-C.; Chen, Y.; Guo, T.; Xia, R.-J.; Tang, X.; He, M.; Xue, W. Correction to: Synthesis and antibacterial activity of novel chalcone derivatives bearing a coumarin moiety. *Chem. Pap.* **2020**, *74*, 4141–4142.

[7]. Hasan, D.; Grinstein, D.; Kuznetsov, A.; Natan, B.; Schlagman, Z.; Habibi, A.; Elyashiv, M. Green Comparable Alternatives of Hydrazines-Based Monopropellant and Bipropellant Rocket Systems. In *Aerospace Engineering*; Dekoulis, G., Ed.; IntechOpen: London, England, 2019.

[8]. Cui, L.; Ji, C.; Peng, Z.; Zhong, L.; Zhou, C.; Yan, L.; Qu, S.; Zhang, S.; Huang, C.; Qian, X.; Xu, Y. Unique tri-output optical probe for specific and ultrasensitive detection of hydrazine. *Anal. Chem.* **2014**, *86*, 4611–4617.

[9]. Dai, X.; Wang, Z.-Y.; Du, Z.-F.; Miao, J.-Y.; Zhao, B.-X. A simple but effective near-infrared ratiometric fluorescent probe for hydrazine and its application in bioimaging. *Sens. Actuators B Chem.* **2016**, *232*, 369–374.

[10]. Manna, S. K.; Gangopadhyay, A.; Maiti, K.; Mondal, S.; Mahapatra, A. K. Recent developments in fluorometric and colorimetric chemodosimeters targeted towards hydrazine sensing: Present success and future possibilities. *ChemistrySelect* **2019**, *4*, 7219–7245.

[11]. Xing, M.; Wang, K.; Wu, X.; Ma, S.; Cao, D.; Guan, R.; Liu, Z. A coumarin chalcone ratiometric fluorescent probe for hydrazine based on deprotection, addition and subsequent cyclization mechanism. *Chem. Commun. (Camb.)* **2019**, *55*, 14980–14983.

[12]. Roy, B.; Bandyopadhyay, S. The design strategies and mechanisms of fluorogenic and chromogenic probes for the detection of hydrazine. *Anal. Methods* **2018**, *10*, 1117–1139.

[13]. Diyali, N.; Chettri, M.; De, A.; Biswas, B. Synthesis, crystal structure, and antidiabetic property of hydrazine functionalized Schiff base: 1,2-Di(benzylidene)hydrazine. *Eur. J. Chem.* **2022**, *13*, 234–240.

[14]. Li, M.; He, J.; Wang, Z.; Jiang, Q.; Yang, H.; Song, J.; Yang, Y.; Xu, X.; Wang, S. Novel nopinone-based turn-on fluorescent probe for hydrazine in living cells with high selectivity. *Ind. Eng. Chem. Res.* **2019**, *58*, 22754–22762.

[15]. Makarovsky, I.; Markel, G.; Dushnitsky, T.; Eisenkraft, A. Hydrazine – The Space Era Agent. *Isr. Med. Assoc. J.* **2008**, *10*, 302–306.

[16]. Desai, K.; Dharaskar, S.; Khalid, M.; Gedam, V. Effectiveness of ionic liquids in extractive–oxidative desulfurization of liquid fuels: a review. *Chem. Pap.* **2022**, *76*, 1989–2028.

[17]. Li, J.; Cui, Y.; Bi, C.; Feng, S.; Yu, F.; Yuan, E.; Xu, S.; Hu, Z.; Sun, Q.; Wei, D.; Yoon, J. Oligo(ethylene glycol)-functionalized ratiometric fluorescent probe for the detection of hydrazine in vitro and in vivo. *Anal. Chem.* **2019**, *91*, 7360–7365.

[18]. Ban, Y.; Wang, R.; Li, Y.; An, Z.; Yu, M.; Fang, C.; Wei, L.; Li, Z. Mitochondria-targeted ratiometric fluorescent detection of hydrazine with a fast response time. *New J Chem* **2018**, *42*, 2030–2035.

[19]. Shi, X.; Yin, C.; Zhang, Y.; Wen, Y.; Huo, F. A novel ratiometric and colorimetric fluorescent probe for hydrazine based on ring-opening reaction and its applications. *Sens. Actuators B Chem.* **2019**, *285*, 368–374.

[20]. Yu, L.; Liu, H.; Liu, X.; Wang, J.; Xu, J.; Wang, H.; Hou, W.; Zhang, H. Multiple detection for hydrazine based on reduction of the 1,6,7,12-tetrachloroperylene diimide derivative. *Chem. Pap.* **2018**, *72*, 1927–1933.

[21]. Yu, S.; Wang, S.; Yu, H.; Feng, Y.; Zhang, S.; Zhu, M.; Yin, H.; Meng, X. A ratiometric two-photon fluorescent probe for hydrazine and its applications. *Sens. Actuators B Chem.* **2015**, *220*, 1338–1345.

[22]. Rao, N.; Le, Y.; Li, D.; Zhang, Y.; Wang, Q.; Liu, L.; Yan, L. A new phenothiazine-based fluorescent probe for detection of hydrazine with naked-eye color change properties. *Chem. Pap.* **2022**, *76*, 267–275.

[23]. John Xavier, S. S.; Siva, G.; Ranjani, M.; Divya Rani, S.; Priyanga, N.; Srinivasan, R.; Pannipara, M.; Al-Sehemi, A. G.; Gnana kumar, G. Turn-on fluorescence sensing of hydrazine using MnO2 nanotube-decorated g-C3N4 nanosheets. *New J Chem* **2019**, *43*, 13196–13204.

[24]. Yang, X.; Liu, Y.; Wu, Y.; Ren, X.; Zhang, D.; Ye, Y. A NIR ratiometric probe for hydrazine "naked eye" detection and its imaging in living cell. *Sens. Actuators B Chem.* **2017**, *253*, 488–494.

[25]. Zhao, J.; Xu, Y.; Li, H.; Lu, A.; Sun, S. A facile intracellular fluorescent probe for detection of hydrazine and its application. *New J Chem* **2013**, *37*, 3849–3852.

[26]. Muhammad, S.; Bibi, A.; Shafiq-urRehman; Bibi, S.; Al-Sehemi, A. G.; Algarni, H.; Sarwar, F. Exploring the quinoidal oligothiophenes to their robust limit for efficient linear and nonlinear optical response properties. *Chem. Pap.* **2022**, *76*, 4273–4288.

[27]. Tandel, S.; Patel, N. C.; Kanvah, S.; Patel, P. N. An efficient protocol for the synthesis of novel hetero-aryl chalcone: A versatile synthon for several heterocyclic scaffolds and sensors. *J. Mol. Struct.* **2022**, *1269*, 133808.

[28]. Saha, S.; Das, S.; Sarkar, O.; Chattopadhyay, A.; Rissanen, K.; Sahoo, P. Introduction of a luminescent sensor for tracking trace levels of hydrazine in insect pollinated cropland flowers. *New J Chem* **2021**, *45*, 17095–17100.

[29]. Liu, L.; Xing, M.; Han, Y.; Zhang, X.; Li, P.; Cao, D.; Zhao, S.; Ma, L.; Liu, Z. Sensing for hydrazine of a pyrene chalcone derivative with acryloyl terminal group. *Spectrochim. Acta A Mol. Biomol. Spectrosc.* **2022**, *264*, 120272.

[30]. Goswami, S.; Paul, S.; Manna, A. Fast and ratiometric "naked eye" detection of hydrazine for both solid and vapour phase sensing. *New J Chem* **2015**, *39*, 2300–2305.

[31]. Tandel, S. N.; Mistry, P.; Patel, P. N. Novel chalcone scaffolds of benzothiophene as an efficient real time hydrazine sensor: Synthesis and single crystal XRD studies. *J. Mol. Struct.* **2023**, *1274*, 134495.

[32]. Cao, Y. W.; Li, X. L.; He, Y. W. A high selective fluorescent sensor for Ni(II) ion in acetonitrile. *Eur. J. Chem.* **2017**, *8*, 314–316.

[33]. Rai, S.; Patel, P. N.; Chadha, A. Preparation, characterisation, and crystal structure analysis of (2E,2′E)-3,3′-(1,4-phenylene)bis(1-(2-aminophenyl)prop-2-en-1-one. *Crystallogr. Rep.* **2016**, *61*, 1086–1089.

[34]. Patel, P. N.; Chadha, A. A simple metal free highly diastereoselective synthesis of heteroaryl substituted (±) cyclohexanols by a branched domino reaction. *Tetrahedron* **2018**, *74*, 204–216.

[35]. Patel, P. N.; Chadha, A. Synthesis, single crystal structure and spectroscopic aspects of Benzo[b]thiophene-3-carbaldehyde based chalcones. *J. Chem. Crystallogr.* **2016**, *46*, 245–251.

[36]. Zhu, Y.; Gong, X.; Li, Z.; Zhao, X.; Liu, Z.; Cao, D.; Guan, R. A simple turn-on ESIPT and PET-based fluorescent probe for detection of Al3+ in real-water sample. *Spectrochim. Acta A Mol. Biomol. Spectrosc.* **2019**, *219*, 202–205.

[37]. Qu, J.; Zhang, Z.-H.; Zhang, H.; Weng, Z.-T.; Wang, J.-Y. Diethyl malonate-based turn-on chemical probe for detecting hydrazine and its bio-imaging and environmental applications with large Stokes shift. *Front. Chem.* **2020**, *8*, 602125.

[38]. Hassaneen, H. M.; Shawali, A. S. Regioselective synthesis of some functionalized 3,4'-bis-(pyrazolyl)ketones and chemoselectivity in their reaction with hydrazine hydrate. *Eur. J. Chem.* **2013**, *4*, 102–109.